NANO LETTERS

Letter

pubs.acs.org/NanoLett

Evidence of Silicene in Honeycomb Structures of Silicon on Ag(111)

Baojie Feng,[†] Zijing Ding,[†] Sheng Meng,[†] Yugui Yao,[‡,†] Xiaoyue He,[†] Peng Cheng,[†] Lan Chen,*[,†] and Kehui Wu*[,†]

[†]Institute of Physics, Chinese Academy of Sciences, Beijing 100190, China

[‡]School of Physics, Beijing Institute of Technology, Beijing 100081, China

ABSTRACT: In the search for evidence of silicene, a two-dimensional honeycomb lattice of silicon, it is important to obtain a complete picture for the evolution of Si structures on Ag(111), which is believed to be the most suitable substrate for growth of silicene so far. In this work we report the finding and evolution of several monolayer superstructures of silicon on Ag(111), depending on the coverage and temperature. Combined with first-principles calculations, the detailed structures of these phases have been illuminated. These structures were found to share common building blocks of silicon rings, and they evolve from a fragment of silicene to a complete monolayer silicene and multilayer silicene. Our results elucidate how silicene forms on Ag(111) surface and provides methods to synthesize high-quality and large-scale silicene.

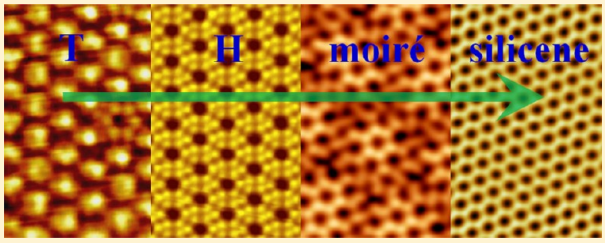

KEYWORDS: *Silicene, Ag(111), scannning tunneling microscopy, molecular beam epitaxy, first-principles calculation*

With the development of the semiconductor industry toward a smaller scale, the rich quantum phenomena in low-dimensional systems may lead to new concepts and ground-breaking applications. In the past decade graphene has emerged as a low-dimensional system for both fundamental research and novel applications including electronic devices, energy storage, and transparent protection layer.[1−4] Inspired by the fruitful results based on graphene, recently a lot of interest has been drawn to group IV (Si, Ge) analogs of graphene.[5−7] It has been theoretically shown that silicene, with Si atoms packed in a honeycomb lattice, like graphene, is a new massless Dirac Fermion system.[5,8] Compared with that of graphene, the stronger spin−orbit coupling in silicene may lead to a detectable quantum spin Hall effect (QSHE) and other attractive properties.[8−11] The compatibility of silicene with silicon-based nanotechnology makes this material particularly interesting for device applications.

As the theoretical studies on silicene are rapidly increasing, the major challenge in this field is now the preparation of high-quality silicene films. However, to date, there is still no solid evidence for the observation of a silicene film. There have been a few works on the formation of silicene nanoribbons on Ag(110) with graphene-like electronic signature.[12,13] The only published work on the preparation of silicene-like sheets was reported by Lalmi et al. on Ag(111).[14] They showed scanning tunneling microscopy (STM) images of a honeycomb monolayer structure that resembles monolayer graphene structure. However, in their experiment the observed lattice constant was about 17% smaller than the theoretically proposed model or the value of bulk silicon. Such a huge compression of the lattice is rather unlikely to be induced by the strain between the film and the substrate. Their results therefore remain to be confirmed and understood. For the purpose of finding evidence of silicene and optimizing the preparation procedure for growing high-quality silicene films, it is important to build a complete understanding of the formation mechanism and growth dynamics of possible silicon structures on Ag(111), which is currently believed to be the best substrate for growing silicene.

In this Letter, we present a systematic study of the self-organized superstructures formed by submonolayer silicon grown on Ag(111), by STM and scanning tunneling spectroscopy (STS). We found that, depending on the substrate temperature and silicon coverage, several monolayer superstructures can form on Ag(111). These superstructures are distinct from any known surface structures of bulk silicon and are characterized by honeycomb building blocks and structures. At sufficiently high temperature and Si coverage, monolayer and multilayer silicene films were grown. Combined with first-principles calculations, the structural models of these phases are proposed, and their evolution with temperature and Si coverage is discussed. Our work provides a complete understanding of the structure evolution of Si on Ag(111), which is desirable for fabrication of high-quality silicene and exploring its novel physics and applications.

Experiments and Methods. Experiments were carried out in a home-built low-temperature STM with a base pressure of 5 × 10^{-11} Torr. Single-crystal Ag(111) sample was cleaned by cycles of argon ion sputtering and annealing. Silicon was evaporated from a heated wafer (≈1200 K) onto the preheated substrate. The deposition rate of silicon was kept at 0.08−0.1

Received: March 17, 2012
Revised: May 29, 2012
Published: June 1, 2012

   dx.doi.org/10.1021/nl301047g | *Nano Lett.* 2012, 12, 3507−3511

ML/min (here 1 monolayer refers to the atomic density of a ideal silicene sheet). The STS data were acquired using a lock-in amplifier by applying a small sinusoidal modulation to the tip bias voltage (typically 10 mV at 676 Hz). All our STM experiments were carried out at 77 K.

First-principles calculations were performed within the framework of density functional theory (DFT) using projected augmented wave (PAW)[15,16] pseudopotentials and the Perdew–Burke–Ernzerholf (PBE)[17] form for exchange–correlation functional, as implemented in Vienna ab initio simulation package (VASP).[18] During calculations, the structures were relaxed without any symmetry constraints using a plane-wave energy cutoff of 250 eV. The convergence of energy is set to 1.0×10^{-4} eV. The relaxation process continues until forces are below 0.01 eV/Å.

Results and Discussions. Silicon atoms deposited on Ag(111) tend to form clusters or other disordered structures when the substrate temperature is below 400 K during growth (data not shown here). As substrate temperature increases to 420 K, two ordered phases form, as shown in Figure 1. The less ordered phase consists of close-packed protrusions (labeled T), and the highly ordered phase exhibits honeycomb structures (labeled H). The two phases can coexist on the surface within a large coverage range, from 0.5 to 0.9 ML (Figure 1a,b, respectively).

The coexistence of phases H and T indicates that these two phases have quite similar formation energy and stability. One can therefore expect similarity and relations between the atomic structure of these two phases. Indeed, the high-resolution STM images in Figure 1c,d show that every big bright protrusion in both phase T and H is indeed composed of three smaller spots that we refer to as a "trimer", although in phase H the trimers are perfectly ordered, while in phase T they exhibit some irregularity and distortion when looked at closely. The two phases share the same periodicity of 1.18 nm, therefore the density of trimers in phase H is just twice of that in phase T. We further performed STS measurements for the two phases (Figure 1e). The dI/dV curves exhibit very similar features of electronic density of states (DOS), which strongly implies that the two phases may share some common building blocks in their atomic structures. In fact, in Figure 1c, there is a noticeable point showing a corner hole and six protrusions surrounding it—a characteristic signature of formation of phase H. Moreover, we notice that phase T prefers to form at a lower Si coverage and a slightly lower temperature as compared with phase H. With the increase of substrate temperature and coverage, phase T decreases in percentage and eventually disappears completely at 460 K. Meanwhile, phase H can spread over the surface if the coverage is sufficiently high. This means that phase H is more stable than phase T, and phase T can be regarded as a precursor state of phase H.

We now face a direct question whether these two phases, especially the well-ordered H phase, are the theoretically proposed silicene. The phase T can be excluded first due to the significantly lower density of Si than that of phase H. We notice that the periodicity of 1.18 nm is almost exactly four times the lattice constant of Ag(111) 1 × 1 surface, 0.29 nm, or three times the lattice constant of silicene, 0.38 nm. Therefore both phases H and T can be written as 4 × 4 reconstruction with respect to the 1 × 1 Ag substrate or 3 × 3 reconstruction with respect to 1 × 1 silicene lattice (in this Letter we refer to as 3 × 3). In fact, Ag/Si system is known as a typical "magic mismatched" system, such that three times the lattice constant

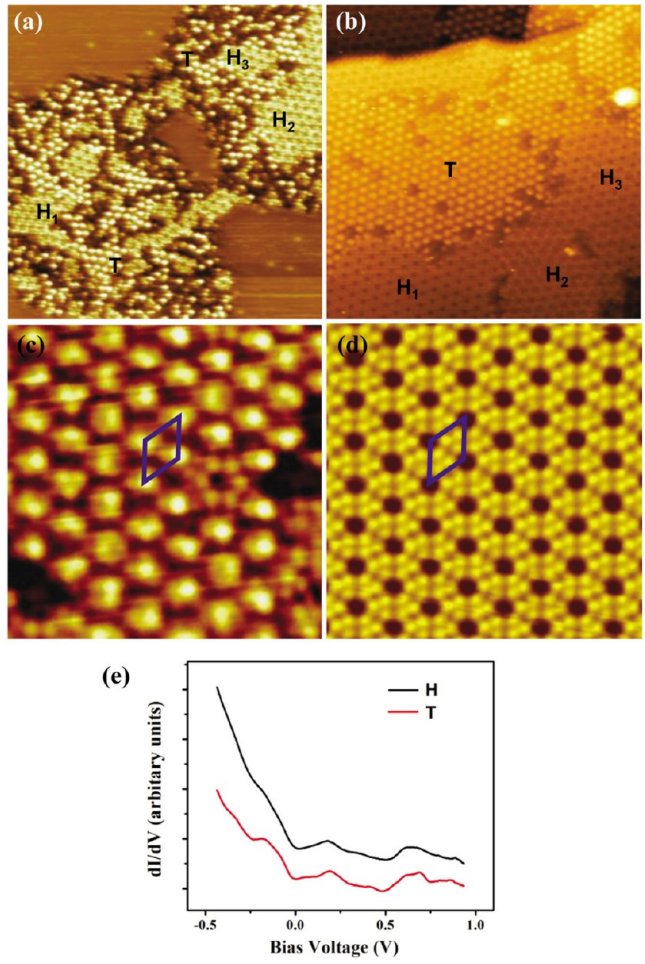

Figure 1. (a) STM image (V_{tip} = 1.2 V) of 0.5 ML silicon atoms deposited on Ag(111) surface at substrate temperature of 420 K. The areas with phase T were marked by "T", while the areas with phase H (with different rotation angles) were marked by H_1–H_3, respectively. (b) STM image (V_{tip} = −1.5 V) of 0.9 ML silicon atoms deposited on Ag(111) surface at substrate temperature of 440 K. The areas of phase T and H are labeled. Notably H_1–H_3 mark areas with phase H in different orientations. (c,d) High-resolution STM images (8.5 × 8.5 nm^2, V_{tip} = −1.0 V) showing the atomic structure of phase T and H, respectively. The blue rhombuses in (c,d) indicate the unit cells of two phases. (e) dI/dV spectra taken at areas of phase T (red) and H (black), respectively. The curves have been shifted vertically for clarity.

of Si equals exactly four times the lattice constant of Ag. If one assume the observed H phase to be the theoretically proposed silicene, it is possible to obtain a 3 × 3 superstructure by placing the silicene lattice in parallel with the 1 × 1 Ag lattice. However, the crucial point in such moiré pattern models is that the periodicity of the superstructure, or essentially the moiré pattern, is strictly linked with the relative orientations of the two overlapping lattices. If one obtain a 3 × 3 moiré pattern in one orientation, it will be impossible to observe the same pattern in another inequivalent crystallographic orientation. However, as we show in Figure 1a, we have observed the formation of 3 × 3 domains on the same Ag terrace, with different orientations which are obviously inequivalent. This simple experimental fact excludes the possibility that the 3 × 3 structure is a silicene lattice placed on 1 × 1 Ag. In another words, the 3 × 3 reconstruction should come from the structure of the overlayer itself, instead of from the commensuration

dx.doi.org/10.1021/nl301047g | Nano Lett. 2012, 12, 3507–3511

between the overlayer and the substrate. It is, however, noticeable that the 3 × 3 reconstruction is most clearly resolved in one major crystallographic orientation, while in other orientations, some irregular distortion of the lattice is seen, which should come from the influence of substrate Ag lattice.

As noted above, the periodicity of 1.18 nm is three times the lattice constant of Si(111), 0.38 nm, which is also close to the calculated lattice constant of silicene.[8] Based on STM observation of the characteristic corner hole structure, we propose a model of phase H as shown in Figure 2a. In this model, the corner holes are due to missing of a hexagonal silicon rings in each 3 × 3 cell of a complete honeycomb silicene structure. This model has been confirmed by first-principles calculations. In the calculation the structure was modeled with low-buckled silicene lattice[8] with missing silicon rings at the corners, and the six Si atoms around the corner are hydrogenated to saturate the Si dangling bond and simplify the calculations. After relaxation, there are no in-plane changes of the position of silicon atoms, but the atoms close to the corner holes (red atoms in Figure 2a) move upward, corresponding well with the trimer feature observed by STM.

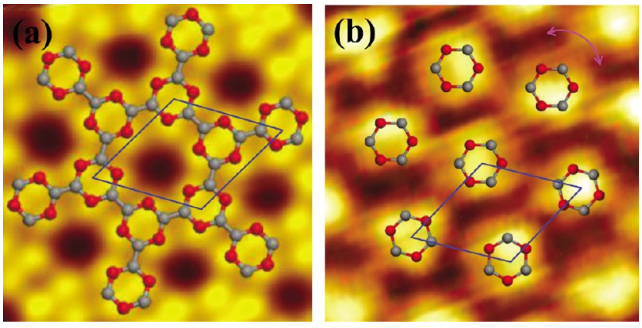

Figure 2. (a,b) High-resolution STM images superposed with calculated model of phase H and T, respectively. The red and gray balls in the models represent buckled and unbuckled silicon atoms, respectively. The blue rhombus in (a) and (b)indicate unit cells as shown in Figure 1(c) and (d). The double arrows indicate that the rings can rotate randomly along their centers.

Based on the atomic structure of phase H, the understanding of the atomic structure of phase T becomes straightforward. Because the STM observation shows that the density of Si trimers in phase T is half of that in phase H, we construct the model of phase T by removing half of the silicon rings in phase H, leaving only one hexagonal silicon ring per 3 × 3 unit cell, as shown in Figure 2b. This model has also been validated by first-principles calculations. Similar to the calculation of phase H, we chose low-buckled silicene rings, saturated by hydrogen atoms as in the original structure. The calculation results show that this model is stable. Each trimer corresponds to a buckled silicon ring with three Si atoms moving upward. Such a structure can be considered as self-assembly of hexagonal silicon rings stabilized by weak van der Waals force and interaction between Si and Ag(111). Compared with the honeycomb arrangement of Si rings connected by covalent bonds in phase H, the weak connection of Si rings in phase T might explain the observed more disordered trimer structure, as compared with the highly ordered trimer structure in phase H.

When the substrate temperature during silicon growth reaches 480 K, the silicon structure exhibits another phase with obvious moiré pattern, which is long-range ordered and can spread over the whole surface as shown in Figure 3a. The

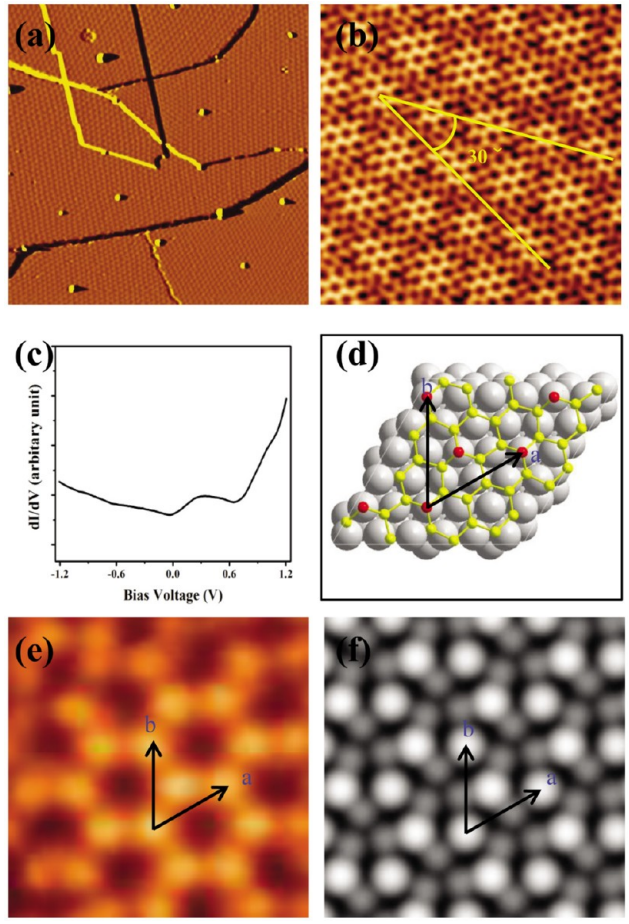

Figure 3. (a) A derivative STM image (200 × 200 nm^2, V_{tip} = 1.43 V) of 0.9 ML silicon atoms deposited on Ag(111) surface at substrate temperature of 480 K. (b) High-resolution STM image (15 × 15 nm^2, V_{tip} = −1.0 V) showing the atomic structure of moiré patterns. The bright areas exhibit complete honeycomb rings with a period of 1.0 nm, while other areas are defective and disordered. The angle between the orientation of the hexagonal rings and the direction of moiré patterns is 30°. (c) dI/dV spectra taken at the moiré pattern phase, in which a peak at 0.3 V and a shoulder at 0.9 V are observed. (d) Calculated model of $\sqrt{7} \times \sqrt{7}$ superstructure of silicene. The gray, yellow, and red balls represent the silver, lower silicon, and higher silicon atoms, respectively. (e,f) Experimental and simulated STM images (1.0 eV above Fermi energy) showing the similar structure features and unit cell of lattice.

orientation of moiré pattern is along the $\langle 1\bar{1}0 \rangle$ direction of Ag(111), and the period is about 3.8 nm. The high-resolution STM image in Figure 3 indicates that a few complete honeycomb rings with lattice period about 1.0 nm are observed at the bright part of the moiré pattern, and the other parts are rather defective and disordered. Additionally the angle between the direction of moiré pattern and honeycomb structure is about 30°. The dI/dV spectra measured on this structure shows a peak at 0.3 V and a shoulder at 0.9 V, which is distinct from that of phase T and H and indicating an essentially different structure formed.

Considering that the complete honeycomb structure with 1.0 nm periodicity is only observed at special positions on surface, we proposed that this honeycomb superstructure consists of fragments of single layer of silicene with strong interaction with the Ag(111) substrate. In order to clarify our supposition, first-principle calculations have been performed. The structure

dx.doi.org/10.1021/nl301047g | *Nano Lett.* 2012, 12, 3507−3511

model is constructed as single layer, low-buckled silicene being in registry with five Ag(111) planes. Except for the two bottom Ag layers, all atoms are relaxed during the geometry optimization. The energetically stable structure is shown in Figure 3d. From the calculation results we find that silicon atoms directly above a silver atom (red balls in Figure 3d) are higher than other silicon atoms. As a result these atoms should be observed as bright protrusions in STM image and forming a $\sqrt{7} \times \sqrt{7}$ superstructure with respect to silicene or $(2\sqrt{3} \times 2\sqrt{3})$R30° superstructure with respect to Ag(111). This gives a larger honeycomb lattice with period $0.386 \times \sqrt{7} = 1.02$ nm, in accordance well with our experimental data. The simulated STM image according to the calculated model is shown in Figure 3f. The similar structure features and lattice period, as observed in experimental STM images (Figure 3e), strongly support our suggested model. Actually there is a slight deviation between the lattice constant of $\sqrt{7} \times \sqrt{7}$ (1.02 nm) superstructure of silicene from that of $2\sqrt{3} \times 2\sqrt{3}$ (1.00 nm) lattice of Ag(111), which result in the formation of the moiré pattern. The optimized structural model in Figure 3d shows the hexagonal rings of silicene are twisted due to the strong interaction between silicon atoms and silver substrate. The bright parts of moiré pattern are where the positions of atoms in silicene are little deviated from that of Ag(111), which make the honeycomb superstructure stable enough to keep the hexagonal rings complete. In other parts of moiré pattern, the larger deviation of position between atoms in silicene and those of Ag(111) lead to unstable honeycomb structure and eventually breaks the hexagonal rings of silicene, resulting in defective and disordered structures. The disordered structures were not obtained in our calculations because the unit cell we choose is much smaller than that of a moiré pattern. The angle between the lattice direction of the $\sqrt{7} \times \sqrt{7}$ superstructure and $\langle 1\bar{1}0 \rangle$ direction of Ag(111) is 30°, so the angle between the direction of moiré pattern and $\langle 1\bar{1}0 \rangle$ direction of Ag(111) should be zero, which has been confirmed by our experiments.

As the substrate temperature reaches 500 K and the coverage is up to 0.8 ML, we observed dense honeycomb structure which we identify as silicene. The STM image in Figure 4a shows a one-atom-thick silicene sheet across the step edges of the Ag(111) surface without losing continuity of the atomic lattice, which is similar to graphene grown on metal surfaces.[19] The high-resolution STM image of Figure 4b shows a honeycomb structure. However, different from the reported 1×1 structure of silicene,[14] the lattice period of the honeycomb structure we observed is about 0.64 nm, which is corresponding to a $\sqrt{3} \times \sqrt{3}$ honeycomb superstructure with respect to the 1×1 silicene lattice. For the general low-buckled silicene model,[8] three Si atoms in one hexagonal ring are upper buckled but still exhibit 1×1 lattice (we named the AB configuration). To explain $\sqrt{3} \times \sqrt{3}$ superstructure, we give a symmetric-buckled silicene model shown in Figure 4c. In this structure model, the six Si atoms in one hexagonal ring are not in plain: two atoms are buckled upward (red atoms in Figure 4c) and one atom is buckled downward (green atoms in Figure 4c), which we named the AB$\bar{\text{A}}$ configuration. The DFT calculations showed AB$\bar{\text{A}}$ configuration with the lattice period determined by our experimental data are more stable than AB configuration (the detail of calculations is shown in ref 20). The upper buckled Si atoms are resolved by STM as the $\sqrt{3} \times \sqrt{3}$ honeycomb superstructure. Based on this model and the lattice constant of silicene in our experiment, the atomic density of silicene is calculated as 1.69×10^{15} cm^{-2}. Different from graphene

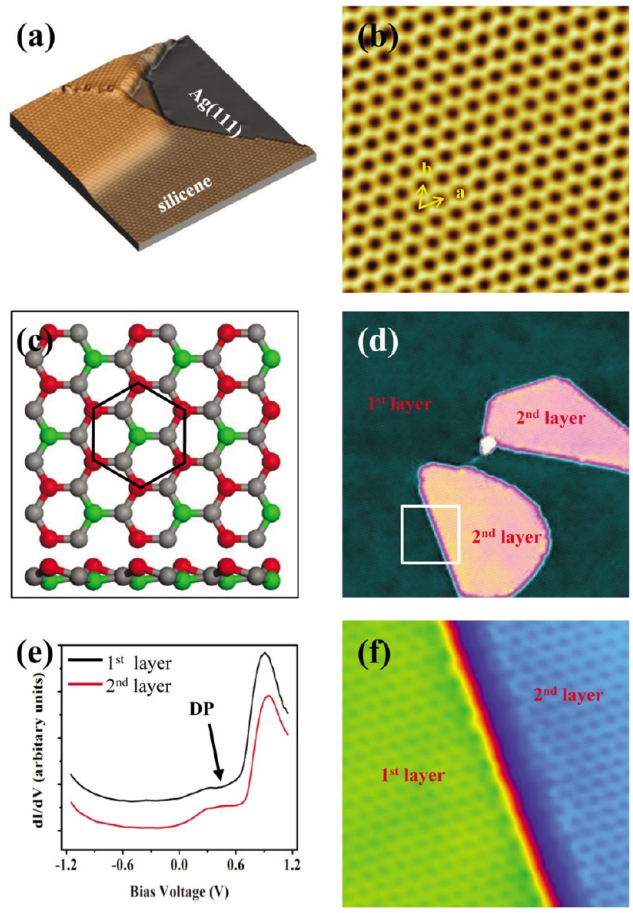

Figure 4. (a) 3D STM image (30×30 nm^2, V_{tip} = 1.0 V) of a single layer of silicene island across a step edge of Ag(111). (b) High-resolution STM image (8×8 nm^2, V_{tip} = 1.2 V) of one monolayer silicene terrace showing the $\sqrt{3} \times \sqrt{3}$ honeycomb superstructure with the period of 0.64 nm. (c) Top and side views of schematic model of $\sqrt{3} \times \sqrt{3}$ superstructure of silicene. The red, gray, and green balls represent the upper buckled, in plain, and lower buckled Si atoms, respectively. The $\sqrt{3} \times \sqrt{3}$ honeycomb superstructure is indicated by the black hexagon. (d) STM image (54×54 nm^2, V_{tip} = 1.5 V) of 1.2 ML silicon atoms deposited on Ag(111) surface at substrate temperature of 500 K showing the second layer of silicene formed on the first layer of silicene. (e) dI/dV spectra taken on the first (black) and second (red) layers of silicene, respectively. (f) High-resolution STM image (10.5×10.5 nm^2, V_{tip} = 1.5 V) of area as marked by the white rectangle in (d) showing atomic structure of the first and second layers of silicene simultaneously.

epitaxially grown on metals,[21,22] we did not observe moiré patterns in our film, which may originate from the weak interaction between silicene and the metal substrate.[23] A typical dI/dV spectrum obtained at the silicene terrace (black curve in Figure 4e) shows a shoulder at 0.3 V and a peak at 0.9 V, which is similar as the LDOS distribution measured on moiré patterns phase. Another remarkable feature is a small dip located at 0.5 eV which is corresponding to the Dirac point (DP) of silicene. The dip is not very obvious compared with that of graphene,[24,25] which is probably due to the pronounced electronic DOS of the underlying Ag(111) substrate superimposed on the dI/dV spectra. The deviation of the energy position of DP from the Fermi energy may stem from the charge transfer from the Ag(111) surface to silicene.

The assignment of the above phase as silicon gets a direct proof by the observation of second layer of silicene at higher

dx.doi.org/10.1021/nl301047g | Nano Lett. 2012, 12, 3507−3511

coverage, as shown in Figure 4d. The high-resolution STM image of Figure 4f shows the atomic structure of the first and second layers silicene simultaneously. It is obvious that the second layer silicene also exhibits a $\sqrt{3} \times \sqrt{3}$ honeycomb superstructure, which indicates that the $\sqrt{3} \times \sqrt{3}$ honeycomb superstructure should originate from free-standing silicene and is not influenced by the Ag(111) surface. This layer-stacked silicon structure is similar to graphite and is a new structural phase of silicon, which may host many novel properties. The dI/dV spectrum on second layer of silicene (red curve in Figure 4e) resembles that on the first layer. This striking similarity between the LDOS of monolayer and the bilayer silicene can also confirm our predation that interactions between the monolayer silicene and Ag(111) are as weak as that between the two silicene layers.

Even at a substrate temperature of about 500 K during growth, silicon atoms tend to form the moiré pattern phase if the coverage of silicon is considerably less than 0.8 ML. This indicates that the atomic density of silicene is higher than that of the moiré pattern phase, which justifies our structural model again. Increasing the substrate temperature to above 600 K, no structure of silicon can be observed anymore, leaving only a bare Ag(111) surface. Furthermore, if the sample of silicene on Ag(111) is annealed up to 600 K, silicene film will also disappear. The upper temperature limit that our silicene film can endure is considerably lower that that of graphene.[22,26,27] This might stem from the weaker interaction between silicene and Ag(111) substrate, as compared with that of graphene on Ir(111) surface.

Conclusion. We have systematically investigated the structure evolution of silicene on Ag(111). With the increase of the substrate temperature, silicon atoms on Ag(111) overcome potential barriers and form some metastable structural phases, such as self-assembled honeycomb building blocks (phase T and H) and incomplete silicene film (moiré pattern structure). The most stable phase, decoupled monolayer and bilayer silicene film, will appear eventually. This work provides methods to fabricate high-quality silicene, which is essential to investigate its novel properties, and brings it closer to the use in nanotechnology and other related areas.

AUTHOR INFORMATION

Corresponding Author

*E-mail: lchen@iphy.ac.cn; khwu@iphy.ac.cn

Notes

The authors declare no competing financial interest.

ACKNOWLEDGMENTS

This work was supported by the NSF of China (Grant nos. 11074289 and 91121003) and the MOST of China (Grant nos. 2012CB921703 and 2009CB929101).

REFERENCES

(1) Geim, A. K.; Novoselov, K. S. *Nat. Mater.* **2007**, *6*, 183−191.
(2) Castro Neto, A. H.; Guinea, F.; Peres, N. M. R.; Novoselov, K. S.; Geim, A. K. *Rev. Mod. Phys.* **2009**, *81*, 109−162.
(3) Pumera, M. *Chem. Rec.* **2009**, *9*, 211−223.
(4) Kim, K. S.; et al. *Nature* **2009**, *457*, 706−710.
(5) Cahangirov, S.; Topsakal, M.; Akturk, E.; Sahin, H.; Ciraci, S. *Phys. Rev. Lett.* **2009**, *102*, 236804.
(6) Kara, A.; Enriquez, H; Seitsonen, A. P.; Lew Yan Voon, L. C.; Vizzini, S.; Aufray, B.; Oughaddou, H. *Surf. Sci. Rep.* **2012**, *67*, 1−18.
(7) Kara, A.; Leandri, C.; Davila, M. E.; Padova, P.; De; Ealet, B.; Oughaddou, H.; Aufray, B.; Lay, G. Le *J. Supercond. Novel Magn.* **2009**, *22*, 259−263.
(8) Liu, C. C.; Feng, W. X.; Yao, Y. G. *Phys. Rev. Lett.* **2011**, *107*, 076802.
(9) Liu, C. C.; Jiang, H.; Yao, Y. G. *Phys. Rev. B* **2011**, *84*, 195430.
(10) Kane, C. L.; Mele, E. J. *Phys. Rev. Lett.* **2005**, *95*, 226801.
(11) Bernevig, B. A.; Hughes, T. L.; Zhang, S. C. *Science* **2006**, *314*, 1757−1761.
(12) Aufray, B.; Kara, A.; Vizzini, S.; Oughaddou, H.; Léandri, C.; Ealet, B.; Lay, G. Le *Appl. Phys. Lett.* **2010**, *96*, 183102.
(13) Padova, P. De; et al. *Appl. Phys. Lett.* **2010**, *96*, 261905.
(14) Lalmi, B.; Oughaddou, H.; Enriquez, H.; Kara, A.; Vizzini, S.; Ealet, B.; Aufray, B. *Appl. Phys. Lett.* **2010**, *97*, 223109.
(15) Vanderbilt, D. *Phys. Rev. B* **1990**, *41*, 7892.
(16) Blöchl, P. E. *Phys. Rev. B* **1994**, *50*, 17953.
(17) Perdew, J. P.; Burke, K.; Ernzerhof, M. *Phys. Rev. Lett.* **1996**, *77*, 3865.
(18) Kresse, G.; Hafner, J. *Phys. Rev. B* **1993**, *47*, 558.
(19) Coraux, J.; N'Diaye, A. T.; Busse, C.; Michely, T. *Nano Lett.* **2008**, *8*, 565−570.
(20) Chen, L.; Liu, C. C.; Feng, B. J.; He, X. Y.; Cheng, P.; Ding, Z. J.; Meng, S.; Yao, Y. G.; Wu, K. H.; *arXiv*:1204, 2642.
(21) Marchini, S.; Günther, S.; Wintterlin, J. *Phys. Rev. B* **2007**, *76*, 075429.
(22) Land, T. A.; Michely, T.; Behm, R. J.; Hemminger, J. C.; Comsa, G. *Surf. Sci.* **1992**, *264*, 261−270.
(23) Sutter, E.; Acharya, D. P.; Sadowski, J. T.; Sutter, P. *Appl. Phys. Lett.* **2009**, *94*, 133101.
(24) Zhang, Y. B.; Brar, V. W.; Wang, F.; Girit, C.; Yayon, Y.; Panlasigui, M.; Zettl, A.; Crommie, M. F. *Nat. Phys.* **2008**, *4*, 627−630.
(25) Zhao, L.; et al. *Science* **2011**, *333*, 999−1003.
(26) Sutter, P.; Flege, J.; Sutter, E. *Nat. Mater.* **2008**, *7*, 406−411.
(27) Yu, Q.; Lian, J.; Siriponglert, S.; Li, H.; Chen, Y. P.; Pei, S. *Appl. Phys. Lett.* **2008**, *93*, 113103.